Temperature influence on the ultrasonic signal acquisition path

L. Svilainis, A. Chaziachmetovas, P. Kabišius

Signal processing department,

Kaunas University o f Technology,

Studentu str. 50, LT-51368 Kaunas, Lithuania

E-mail:linas.svilainis@ktu.lt

Abstract

It is important to estimate the group delay time in systems where signal delay is used to extract the measured parameter. In this article the ultrasonic flow measurement system is analyzed. Measurement is carried out using ultrasonic signal, which travels along and against the measured flow. The pulsed delay time measurement technique is used. The system is synchronized by a quartz oscillator. A digital pulse former is used to excite the high voltage generator which in turn delivers the signal to ultrasonic transducer. The transducer is sending the acoustical pulse into liquid in measurement channel. This pulse is received by the transducer at the opposite channel end and converted into electrical signal. This is amplified, filtered and delivered into analog to digit converter. The goal of this investigation was to estimate the temperature influence on the group delay time of the system discussed above. Electrical models have been developed in PSPICE, simulation carried out. Theoretical analytical expressions of the delay time influence on a flow speed estimation are presented.

Temperature influence of individual units was investigated experimentally. Experimental results are presented in numerical and graphical form. It has been concluded that the high voltage generator output stage has the highest temperature sensitivity on delay time among electronics units. But according to the analytical expressions, this influence can be compensated. Then the largest electronics contribution on the group delay time is due to the analog filters present in the signal path.

Keywords: Ultrasonic transit time flow meter, time-of-flight estimation, ultrasound electronics, fuel consumption monitoring.

Introduction

Ultrasound application in measurements became popular because of equipment size, non-destructive, non-invasive nature, environmental safety and cost-effectiveness. Increasing popularity of digital ultrasonic systems is justified by improved accuracy and adaptability of computerized processing. Majority of ultrasonic measurement systems explore the signal delay information: food processing [1], thickness meters [2], flow meters [3], NDE systems [4], temperature meters [5], biomedicine [6, 7] or load measurement [8]. One of the tasks accomplished by such systems is to define the Time-of-flight (ToF) of the ultrasonic signal. Usually matched filter is used for signal-to-noise (SNR) improvement. Then cross-corelation maximum can be used as *ToF* estimate. Random errors produced under such procedure have been analyzed in our previous work [9, 10].

In this paper we are analyzing the ultrasonic transit time flow meter structure, evaluating the influence of separate components on a signal temporal delay.

Flow velocity estimation procedure

The ultrasonic transit time flow meter is exploiting the acoustical signal drag by flow. The ultrasonic beam is supposed to be matched with flow axis. In such case the signal travel time ToF_{up} against the flow will be longer because the ultrasound propagation speed c will be counteracted by flow velocity V [11, 12]:

$$ToF_{up} = \frac{L}{c-V}, \quad (1)$$

where L is the distance between ultrasonic transducers. Then signal travel time ToF_{dn} down the flow will be shorter because the ultrasound propagation speed will be increased by the same direction flow:

$$ToF_{dn} = \frac{L}{c+V}. \quad (2)$$

Then the flow velocity can be obtained if the distance L and the transit times ToF_{up} and ToF_{dn} are available:

$$V = \frac{L(ToF_{up} - ToF_{dn})}{2 \cdot ToF_{up} \cdot ToF_{dn}}. \quad (3)$$

Actually, getting the right *ToF* value is complicated: usually transit times are the combined delay of the whole system [13]. The explanation below is dealing with this question. Let's assume the connection diagram presented in Fig.1.
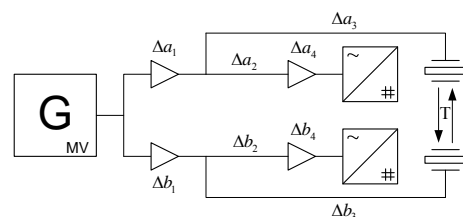

Fig. 1. **Connection diagram for a flow meter**

Two ultrasonic transducers were placed at L distance and signals obtained look like the ones presented in Fig.2.

Two distinct signatures can be indicated in ADC data in Fig.2: i) signature from exciting signal penetration into its own channel (at the beginning of the trace) and ii) signature of opposite channels pulse, traveled along the measuring channel and picked up by the opposite end transducer. Let's analyze how signal travels according the Fig.1 setup.
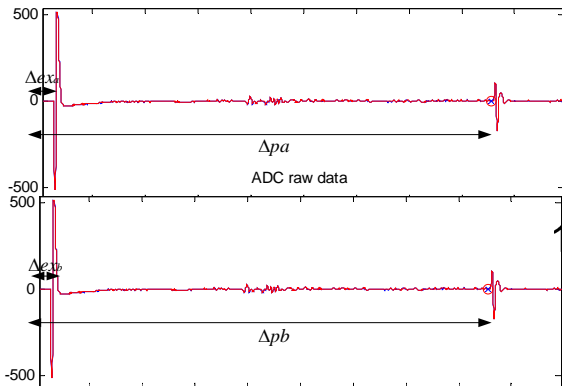
Fig. 2. **Signals recorded by ADC**

High voltage pulser signals were delivered to both transducers simultaneously. Separation was achieved by use of pulse expanders two parallel opposite connected ES1P diode pairs. Pulser logic and synchronization delay the signal by Δg. Expanders delay the signal by value Δa_1 and Δb_1 correspondingly for channels 1 and 2. The signal expanders at the output is split into transducer and reception amplifiers. Cables delivering the signal attribute the delays Δa_2 Δb_2 (to reception) and Δa_3 Δb_3 (to transducer). The amplifier with limiter and filters attribute Δa_4 Δb_4 delays. The delays in acoustic channel can be attributed by the delay ToF_{up} or ToF_{dn} (labeled as „T").

The delay in trigger signal propagation through the pulser, cables and amplifier of the same channel input is Δtx_a Δtx_b:

$$\Delta tx_a = \Delta g + \Delta a_1 + \Delta a_2 + \Delta a_4 , \qquad (4)$$

$$\Delta tx_b = \Delta g + \Delta b_1 + \Delta b_2 + \Delta b_4 . \qquad (5)$$

The trigger signal path through the pulser, cables, ultrasonic channel, reception cables and amplifier of the opposite channel input delay is Δrx_a Δrx_b for first and second channels correspondingly:

$$\Delta rx_a = \Delta g + \Delta b_1 + \Delta b_3 + T + \Delta a_3 + \Delta a_2 + \Delta a_4 , \quad (6)$$

$$\Delta rx_b = \Delta g + \Delta a_1 + \Delta a_3 + T + \Delta b_3 + \Delta b_2 + \Delta b_4 . \qquad (7)$$

There are two ways to obtain the *ToF* value: correlation is obtained between the excitation signal's signature and the opposite channel's propagated signal; or the same channel excitation signal signature and the propagated signal. This is not the true *ToF*, purely attributed by measuring chamber so we label it Δt_{up} and Δt_{dn}. In the first case (opposite channel's signatures) *ToF* is:

$$\Delta t_{up} = \Delta rxb - \Delta txa , \qquad (8a)$$

$$\Delta t_{dn} = \Delta rxa - \Delta txb . \qquad (8b)$$

In second case (same channel's signatures) *ToF* is:

$$\Delta t_{up} = \Delta rxb - \Delta txa , \qquad (9a)$$

$$\Delta t_{dn} = \Delta rxa - \Delta txb . \qquad (9b)$$

Two techniques will differ in which delays are eliminated from the velocity calculation. After combination with Eq. 3 in the first case components with index 2,3 and 4 remain; in the second case components with index 1 and 3 remain. Full equations are too clumsy. For the illustration we present the simplified case below:

there is no flow and only difference between Δt_{up} and Δt_{dn} is calculated:

$$\Delta t1 = 2(\Delta a_2 - \Delta b_2 + \Delta a_4 - \Delta b_4) , \qquad (10)$$

$$\Delta t2 = 2(\Delta b_1 - \Delta a_1) . \qquad (11)$$

If generator part of errors is prevailing, then it is recommended to use the first technique (opposite channels signatures). If reception channel has larger errors then the second technique is preferred (same channel).

The aim is to carry the measurements of fuel flow in trucks. The direct fuel flow rate is within 10…200 l/h. The diameter of the hose is 8 mm; this equals to 50 mm^2. Then the mean flow velocity is 0.05…1.1 m/s. It can be assumed that the flow profile will always be laminar. Then the maximum velocity at the pipe center will be 0.1…2.2 m/s. This results in 25:1 turn-down ratio (1 % expanded uncertainty is desired).

Eq. 3 can be used to get the *ToF* influence on *V* estimation. Sensitivity coefficients are obtained as partial derivatives:

$$\kappa_{tup} = \frac{\partial V}{\partial ToF_{up}} = \frac{L}{2 \cdot ToF_{up}^2} ; \kappa_{tdn} = \frac{L}{2 \cdot ToF_{dn}^2} . \quad (12)$$

Then, assuming that both transit times ToF_{up} and ToF_{dn} are almost equal (flow velocity is only 0.1 %) and have the same variability, the deviation σ_{ToF} in flow velocity value caused by deviation in *ToF* value σ_t can be obtained

$$\sigma_V = \kappa_{tup} \cdot \sqrt{2} \cdot \sigma_t = \sigma_t \frac{L}{\sqrt{2} \cdot ToF_{up}^2} , \qquad (13)$$

Or, it can be reversed for *ToF* accuracy requirements:

$$\sigma_t = \sigma_V \frac{\sqrt{2} \cdot ToF_{up}^2}{L} , \qquad (14)$$

As it was mentioned abovethe *ToF* value is obtained through correlation between the excitation signal's signature and the opposite channel's propagated signal; or the same channel excitation signal signature and the propagated signal. This is not the true *ToF* purely attributed by flow. Furthermore, this delay is not constant with environment parameters and first of all with temperature. Our goal here was to estimate the order of the influence on these delay times by separate system components. For the ultrasound path length *L*=0.1 m the required *ToF* errors should not exceed 40 ps for a minimum flow and 800 ps for the maximum. Taking the 95 % confidence interval 20 ps the *ToF* estimation standard uncertainty for a minimum flow and 400 ps for a maximum are required.

Measurement system structure

In general, a flow meter needs the excitation signal, reception channel, acquisition block and processing and indication units. In order to measure the up- and down-stream transit times simultaneously, two transmission and two reception and acquisition channels are needed which should work in parallel (Fig.3).

If multiple measurement beams are used, then the number of channels is increased.

Transducer excitation waveforms analysis in [14] indicates that the exciting pulse must have the bandwidth

Fig 3. **Simplified system structure**
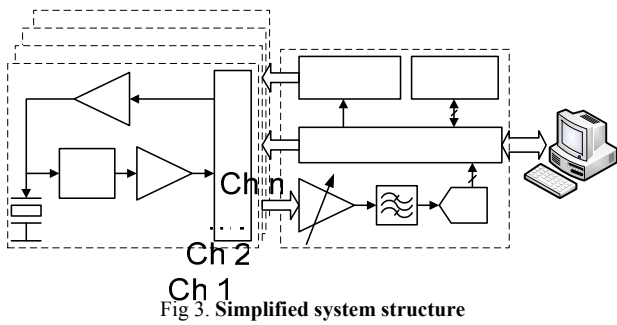
greater or equal the transducer bandwidth. Usually, the bandwidth is desired to be as wide as possible if the temporal resolution is the goal. Also, a wide excitation bandwidth will be least affected by temperature effects due to sharp signal fronts. The conclusion has been made that a rectangular pulse is best matching the bandwidth and efficiency requirements. Of course, in the case of a rectangular pulse, active elements' saturation is limiting the switching speed when there is a need to switch it off for a returning pulse front. Pulse transition time limitations will add additional decay of 20 dB / decade on all power spectra. If wide exciting pulse frequency range is necessary then the step function is a possible candidate (in addition it is easy to generate). The design of the pulser is complicated by a high electrical impedance of an ultrasonic transducer – a high voltage is needed to supply the sufficient power. The most common high voltage pulser is using a high voltage source and two switches connected in totem-pole (Fig. 4).

Fig. 4. **Simple high voltage pulser structure**
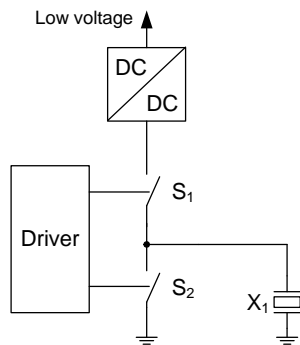
To produce a high voltage on the transducer terminals the switch S_1 is turned on and S_2 stays off. To remove this high voltage from the transducer terminals the S_2 is turned on and S_1 off.

The all operation is controlled by logics. Temperature will have its effect on the logic ICs delay. Simulation or experimental investigation has to be carried out to evaluate how the delay in pulse will depend on temperature.

A low noise preamplifier is used for signal reception [15]. As it was discussed above, the same ultrasonic transducer has to be used for signal transmission and reception. Therefore both excitation and reception signals will be present here (Fig.5). Therefore the preamplifier must contain protection circuit which protects the input against the high voltage excitation pulse.


Fig.5. **Both excitation and resulting signals are present**
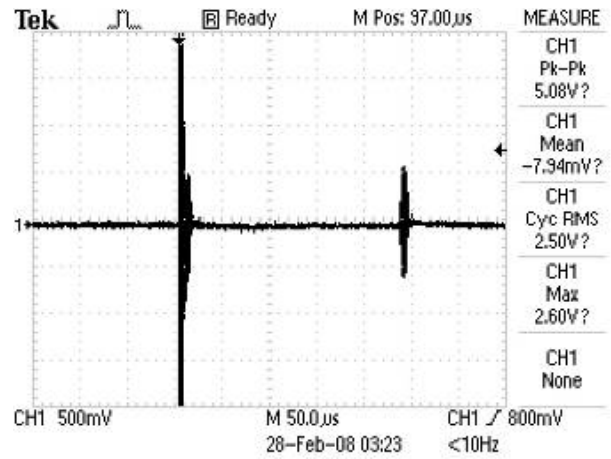
Circuit for such protection is presented in Fig.6. The preamplifier operating in a pulse-echo mode was investigated in [15].

This time situation is slightly different [16]: the ultrasonic transducer is picking up the signals sent by another transducer located at the opposite end on the measurement channel. But we consider situation fully equivalent and therefore only need the analysis of the group delay time behavior.

Fig. 6. **Preamplifier including input limiter circuit**
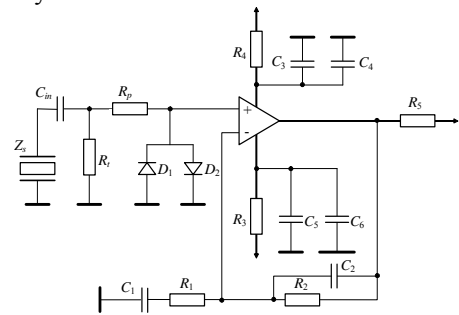
AC parameter measurement system was developed to investigate the group delay. The system (Fig.7) contains both the excitation and the receiving units. The excitation generator is using the direct digital synthesizer (DDS). Thanks to DDS the fixed fraction is established between excitation and acquisition. Therefore the frequency mismatch induced errors are reduced and amplitude and phase measurement improved thanks to the sine wave correlation (SWC) technique [17].

Fig. 7. **Insertion gain measurement system**
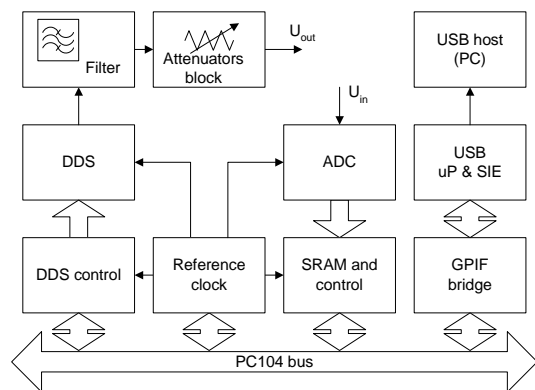
The results for gain and phase measurement are presented in Fig.8. Several candidate amplifiers have been measured.
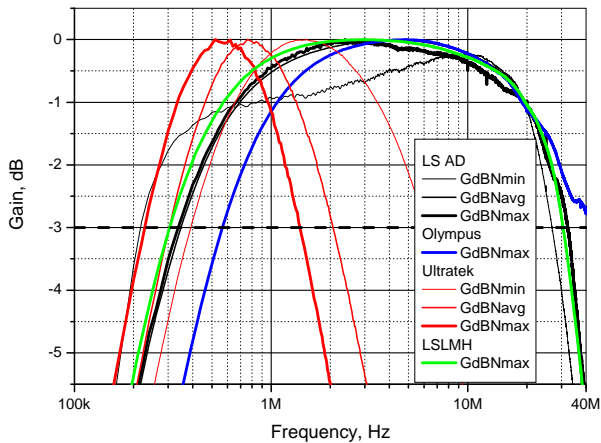

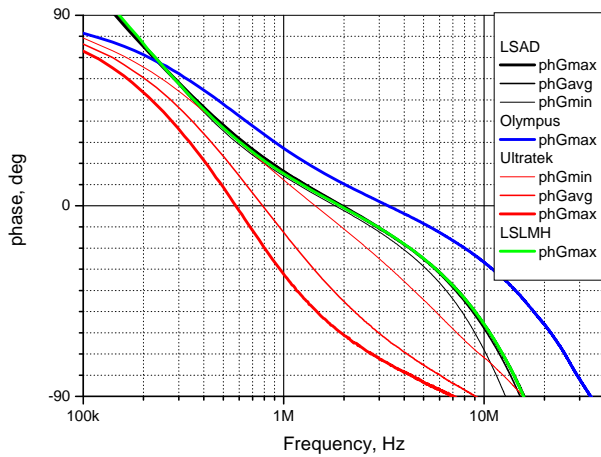Fig. 8. **Premplifier gain AC response**

Fig. 9. **Premplifier phase AC response**

Actually, we are not interested in gain, we need the phase response $\varphi(\omega)$ since the derivative of phase will give the group delay time (GDT) τ_g:

$$\tau_g = -\frac{\partial\varphi(\omega)}{\partial\omega}, \qquad (15)$$

Another unit in a signal path is the analog-to-digit converter (ADC). Aperture delay t_A is the manufacturer specified parameter influencing the time delay, but there is no indication how it depends on temperature.

ADC and pulser logics part are synchronized from the same reference quartz oscillator. Therefore the oscillator stability is also important.

Experiments

To summarize, the following units have to be evaluated for temperature influence: quartz oscillator, pulser control logic, pulser high voltage amplifier, preamplifier with filters and ADC. The infrared non-contact thermometer CA879 with the laser aimer from Chauvin Arnoux was used for the temperature measurement. It has 0.1 ^{o}C resolution, 1.5 % accuracy, 400 ms response time. The surface emissivity of 0.95 was used. Halogen 60 W lamp was used as a non-contact heating element. Experiments were carried out with rising temperature (lamp on) and with decreasing temperature.

The first carried out experiment was the reference oscillator drift with temperature. The system operation is synchronized by 100 MHz 100 ppm reference oscillator. The DDS output (Fig. 7) programmed for 10 MHZ was used to deliver the signal to the Agilent N9320A RF Spectrum Analyzer, 9 kHz - 3 GHz. The frequency span was set 100 Hz, the resolution bandwidth was 10 Hz. Signal peak position was registered and temperature measured in the oscillator case manually. The results are presented in Fig. 10.
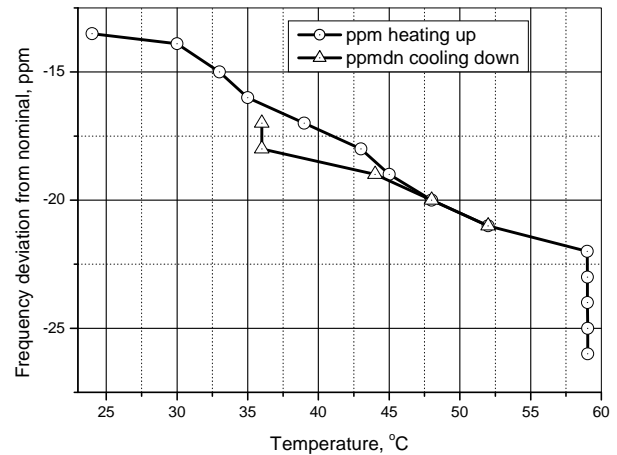

Fig. 10. **Reference oscillator frequency drift vs. temperature**

The experimental system for transducers excitation and simultaneous up-stream and down-stream signals acquisition has been developed (Fig. 6). The system contains pulser control logic (5 ns…2000 ns programmable duration), pulser output power stage with programmable high voltage (0 V…500 V) DC/DC regulated power supply, pulse expander, high bandwidth, high slew rate low noise amplifier with signal protection (+/- 0.5 V) and filtering circuits (0.5 MHz…30 MHz Butterworth 3-rd order), dual channel programmable sampling frequency (12.5 Ms/s, 25 Ms/s, 50 Ms/s and 100 Ms/s) 10 bit flash ADC with buffer memory and glue logic, high speed USB2 interface and data host PC used for collection, storage and processing of acquired data.

The pulser control logic temperature drift was investigated then. The pulser output is used to drive the high voltage pulser. Instead, logic output was delivered to ADC input directly. The signals recorded were filtered using matched filter: the first experiment (no external heat source) one A-scan signal was recorded as the reference and the rest of experiments used 200 A-scans for cross correlation processing. These results were processed for a standard deviation (random errors) and mean value processing. Every new A-scan was followed by temperature manual registration. The procedure was repeated until a notable process stabilization was achieved. Then, the heat source was turned off and the process recorded in opposite temperature change direction. The results for heat-up and cool-down are presented in Fig.11.
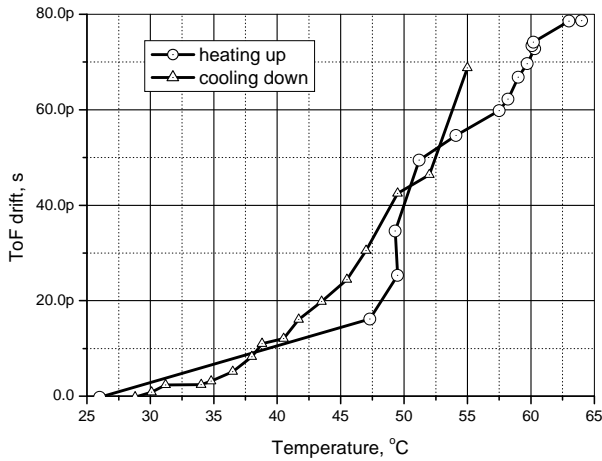
Fig. 11. ***ToF* drift caused by pulser control logic heating**

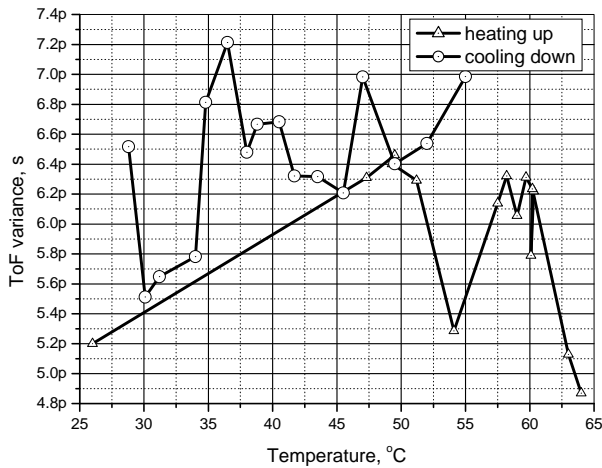Random errors were investigated using the standard deviation of the ToF obtained during experiments (Fig.12).

Fig. 12. **ToF random errors change caused by pulser control logic temperature change**

No notable correlation of random *ToF* errors with the pulser control logic temperature was registered.

Next experiment investigated the high voltage pulser temporal stability. The pulser output through 60 dB attenuator was delivered to the ADC input directly. The signals recorded were filtered using matched filter: the first experiment (no external heat source) - one A-scan signal was recorded as the reference and the rest of experiments used 200 A-scans for cross correlation processing. These results were processed for a standard deviation (random errors) and mean value processing. Every new data packet was followed by automated temperature registration. The procedure was repeated until a notable process stabilization was achieved. Then, the heat source was turned off and the process recorded in opposite temperature change direction. The results for heat-up and cool-down are presented in Fig.13.

There is a significant change in *ToF* when heating up the pulser. The reason is that a high slew rate is used here: 500 V level is reached in roughly 5ns; this corresponds to 100 000 V/us; compare to the best case of 5000 V/us for

operational amplifiers. Random errors were investigated using the standard deviation of the *ToF* obtained during experiments (Fig.14).
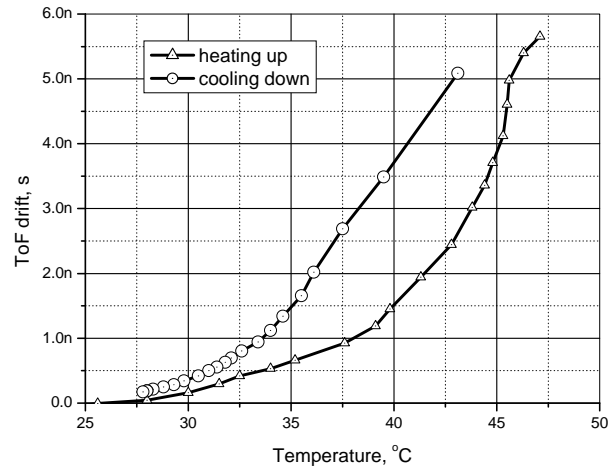

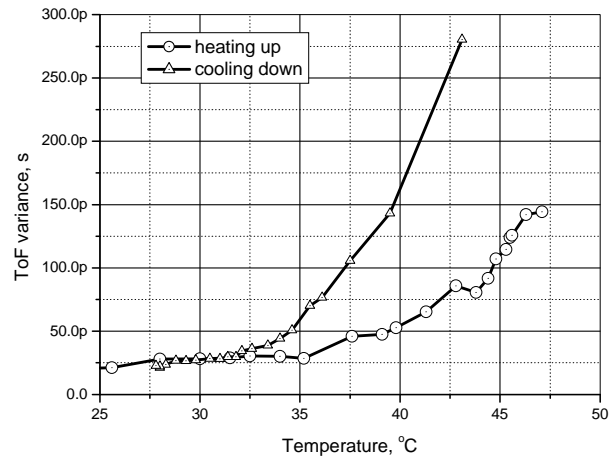
Fig. 13. ***ToF* drift caused by high voltage pulser heating**

Fig. 14. ***ToF* random errors caused by high voltage pulser temperature change**

There is also notable variation in random errors with the high voltage pulser temperature. Fortunately, the same generator is used for both channels for excitation (refer Fig.1) so none of these errors recorder will propagate into the measurement result.

The next experiment investigated temporal stability of the amplifier with limiter and filters. The pulser control logic output through 10 dB attenuator was delivered to the ADC input directly. The signals recorded were filtered using a matched filter: the first experiment (no external heat source) was recorded as the reference and the rest of experiments used 200 A-scans for cross correlation processing. The results were processed for random errors and mean value. Every new data packet was followed by a temperature registration. The procedure was repeated until notable process stabilization was achieved. After the heat source was turned off the process was recorded in opposite temperature change direction. The results for heat-up and cool-down are presented in Fig.15.

There is a moderate change in *ToF* when heating up the amplifier. We attribute that to the filters used. The

random errors were investigated using the standard deviation of the *ToF* obtained during the experiments (Fig.16).
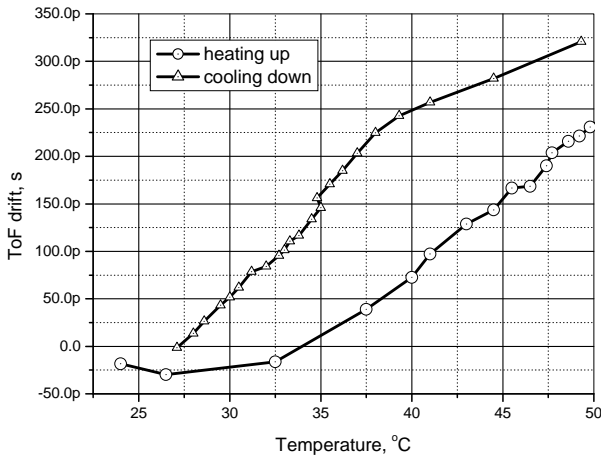

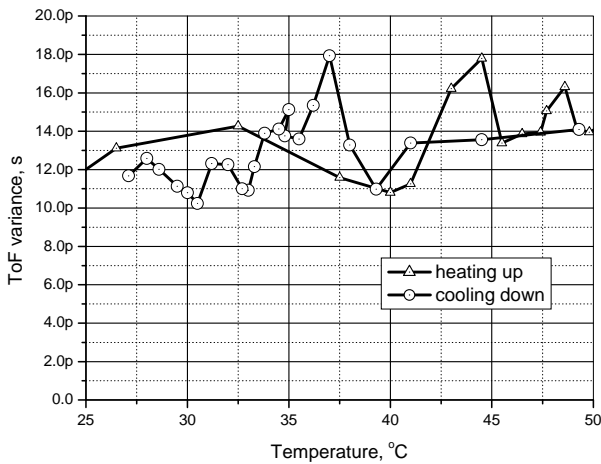Fig. 15. ***ToF* drift caused by high voltage pulser heating**

Fig. 16. ***ToF* random errors caused by high voltage pulser temperature change**

No notable correlation of random *ToF* errors with the amplifier temperature was registered. Additionally, the amplifier AC response was measured. In particular, the gain (Fig.17) and the phase (Fig.18) were investigated at two extreme temperatures: 27°C and 50°C.
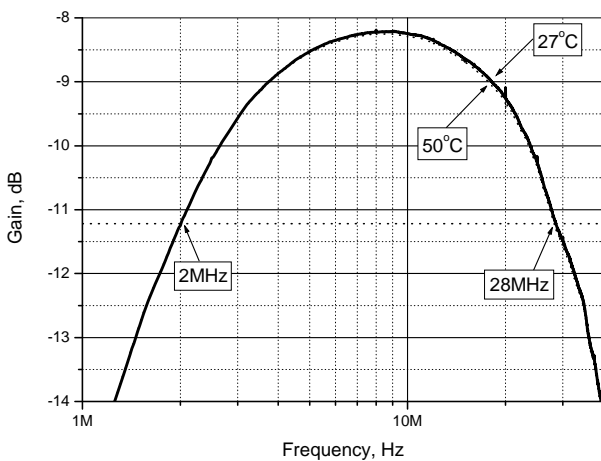

Fig. 17. **Amplifier gain AC response at minimum gain**

There is no notable change in the gain or the phase AC response with temperature. Eq. 15 was used to obtain the GDT of the amplifier (Fig.19).
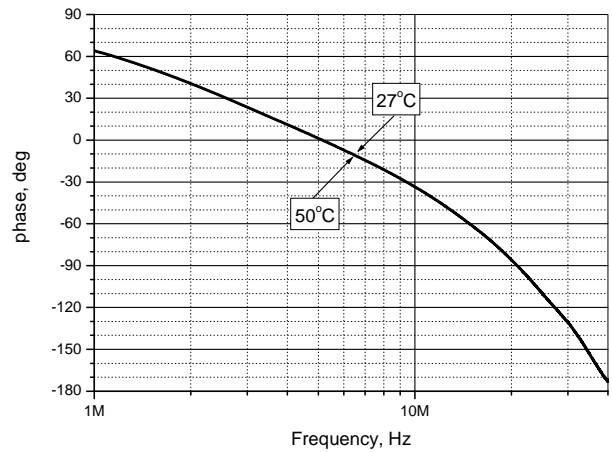

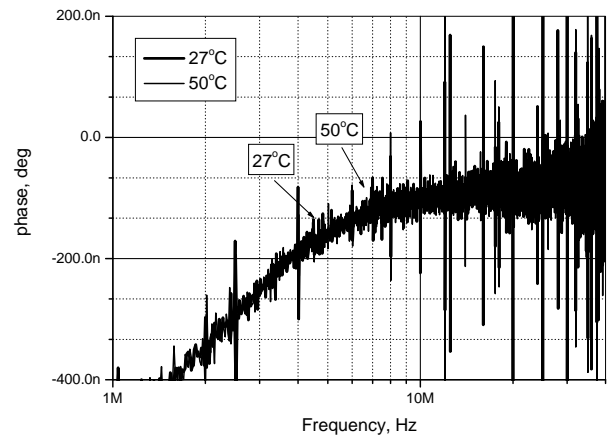Fig. 18. **Amplifier phase AC response at two temperatures**

Fig. 19. **Amplifier GDT AC response at two temperatures**

There is no notable change in GDT with temperature.

Conclusions

It has been concluded that a high voltage generator output stage has the highest temperature sensitivity on the delay time among electronics units. But according t the analytical expressions this influence can be compensated. Then the largest electronics contribution to the group delay time is due to the analog filters present in the signal path.

References

1. **Telis-Romero J., Váquiro H. A., Bon J., Benedito J.** Ultrasonic assessment of fresh cheese composition. Journal of Food Engineering. 2011. Vol. 103(2). P.137-146.

2. **Luciano N. B., Alberto S. C. J. et al.** Development of an ultrasonic thickness measurement equipment prototype. Conference on Electronics, Communications and Computer. 2010. P. 124 – 129.

3. **Magori V.** Ultrasonic measuring arrangement for differential flow measurement, particularly for measurement of fuel consumptions in motor vehicles with a fuel return line. US patent No 4. 409,847. 1983.

4. **Wen-Yuan Tsai et al.** New implementation of high-precision and instant-response air thermometer by ultrasonic sensors. Sensors and Actuators A: Physical. 2005. Vol. 117(1). P. 88-94.

5. **Katouzian A., Sathyanarayana et al.** Challenges in Atherosclerotic Plaque Characterization With Intravascular Ultrasound (IVUS): From Data Collection to Classification. IEEE Transactions on Information Technology in Biomedicine. 2008. Vol. 12(3). P. 315 – 327.

6. **Voleisis A., Kazys R. et al.** Ultrasonic method for the whole blood coagulation analysis. Ultrasonics. 2002. Vol. 40(1-8). P. 101-107.

7. **Draudvilienė L., Mažeika L.** Analysis of the zero-crossing technique in relation to measurements of phase velocities of the S0 mode of the Lamb waves. Ultragarsas. 2010. Vol. 65. No. 3. P.11-14.

8. **Svilainis L.** Temperature effect elimination in ultrasound aided load measurement for ZnO sputtered transducers. Electronics and electrical engineering. 1996. Vol. 8(4). P.49-55.

9. **Svilainis L., Dumbrava V.** The time-of-flight estimation accuracy versus digitization parameters. Ultragarsas. 2008. Vol. 63(1). P.12-17.

10. **Svilainis L., Dumbrava V.** Analysis of the interpolation techniques for time-of-flight estimation. Ultragarsas. 2008. Vol. 63(4). P. 25-29.

11. **Crabtree M. A.** Industrial flow measurement. University of Huddersfield. June 2009.

12. **Kažys R.** Neelektrinių dydžių matavimas. Kaunas: Vitae Litera, 2007.

13. **Eren H.** Accuracy in real time ultrasonic applications and transit-time flow meters. IEEE Instrumentation and Measurement Technology Conference. IMTC/98. 1998. P. 568 - 572.

14. **Svilainis L., Puodžiūnas V.** Ultrasonic NDE system: the hardware concept. Ultragarsas. 1998. Vol. 29(1). P.34-40.

15. **Svilainis L., Dumbrava V.** Investigation of a preamplifier noise in a pulse-echo mode. Ultragarsas. 2005. Vol. 56(3). P. 26-29.

16. **Canqian Y., Kummel M.; Søeberg H.** A transit time flow meter for measuring milliliter per minute liquid flow. Review of Scientific Instruments. 1988. Vol. 59(2). P. 314 – 317.

17. **Svilainis L.** The AC parameters measurement system for ultrasonics. Ultragarsas. 2006. Vol. 60(3). P. 44-48.

L. Svilainis, A. Chaziachmetovas, P. Kabišius

Temperatūros įtakos signalo surinkimo traktui analizė

Reziumė

Matavimo sistemose, kurios naudoja signalo vėlavimą informacijai apie matuojamą parametrą gauti, svarbu įvertinti signalo grupinio vėlinimo laiką. Straipsnis nagrinėja ultragarsinę sistemą, skirtą skysčio srautui matuoti. Matuojama naudojant ultragarsinį signalą, kuris siunčiamas išilgai ir prieš matuojamąjį srautą. Taikomas impulsinis signalo sklidimo laiko matavimo būdas. Sistemos darbas sinchronizuojamas kvarciniu generatoriumi. Skaitmeninis impulsų formuotuvas valdo aukštosios įtampos generatorių, kurio signalas patenka į ultragarsinį keitiklį ir į skystį. Signalą priima kitame kanalo gale esantis ultragarsinis keitiklis. Toliau signalas stiprinamas, filtruojamas ir tada patenka į skaitmeninį analogo keitiklį. Tyrimo tikslas buvo įvertinti temperatūros įtaką aptartų sistemos mazgų grupiniam vėlinimo laikui. Sudaryti elektronikos mazgų PSPICE modeliai, atlikti modeliavimo eksperimentai. Pasiūlytos teorinės analitinės išraiškos signalo vėlinimo laiko įtakai srauto matavimo rezultatui įvertinti.

Atlikti eksperimentai temperatūros įtakai tam tikriems mazgams įvertinti. Rezultatai pateikiami skaitine ir grafine išraiška. Nustatyta, kad iš elektroninių mazgų didžiausia priklausomybe nuo temperatūros pasižymėjo aukštos įtampos generatoriaus galinis laipsnis. Tačiau, kaip rodo analitinės analizės rezultatai, ši įtaka yra kompensuojama. Tuomet didžiausią temperatūros įtaką grupiniam vėlinimo laikui sąlygoja priėmimo trakte esantys analoginiai filtrai.